61. Axions and Other Similar Particles

Revised October 2017 by A. Ringwald (DESY), L.J Rosenberg and
G. Rybka (U. of Washington).

61.1. Introduction

In this section, we list coupling-strength and mass limits for light neutral scalar or pseudoscalar bosons that couple weakly to normal matter and radiation. Such bosons may arise from a global spontaneously broken U(1) symmetry, resulting in a massless Nambu-Goldstone (NG) boson. If there is a small explicit symmetry breaking, either already in the Lagrangian or due to quantum effects such as anomalies, the boson acquires a mass and is called a pseudo-NG boson. Typical examples are axions (A^0) [1,2], familons [3] and majorons [4], associated, respectively, with a spontaneously broken Peccei-Quinn, family and lepton-number symmetry.

A common characteristic among these light bosons ϕ is that their coupling to Standard-Model particles is suppressed by the energy scale that characterizes the symmetry breaking, *i.e.*, the decay constant f. The interaction Lagrangian is

$$\mathcal{L} = f^{-1} J^\mu \partial_\mu \phi \,, \tag{61.1}$$

where J^μ is the Noether current of the spontaneously broken global symmetry. If f is very large, these new particles interact very weakly. Detecting them would provide a window to physics far beyond what can be probed at accelerators.

Axions are of particular interest because the Peccei-Quinn (PQ) mechanism remains perhaps the most credible scheme to preserve CP in QCD. Moreover, the cold dark matter of the universe may well consist of axions and they are searched for in dedicated experiments with a realistic chance of discovery.

Originally it was assumed that the PQ scale f_A was related to the electroweak symmetry-breaking scale $v_{\mathrm{weak}} = (\sqrt{2} G_{\mathrm{F}})^{-1/2} = 247$ GeV. However, the associated "standard" and "variant" axions were quickly excluded—we refer to the Listings for detailed limits. Here we focus on "invisible axions" with $f_A \gg v_{\mathrm{weak}}$ as the main possibility.

Axions have a characteristic two-photon vertex, inherited from their mixing with π^0 and η. This coupling allows for the main search strategy based on axion-photon conversion in external magnetic fields [5], an effect that also can be of astrophysical interest. While for axions the product "$A\gamma\gamma$ interaction strength $\times$ mass" is essentially fixed by the corresponding π^0 properties, one may consider a more general class of axion-like particles (ALPs) where the two parameters (coupling and mass) are independent. A number of experiments explore this more general parameter space. ALPs populating the latter are predicted to arise generically, in addition to the axion, in low-energy effective field theories emerging from string theory [6]. The latter often contain also very light Abelian vector bosons under which the Standard-Model particles are not charged: so-called hidden-sector photons, dark photons or paraphotons. They share a number of phenomenological features with the axion and ALPs, notably the possibility of hidden photon to photon conversion. Their physics cases and the current constraints are compiled in Ref. [7].

61.2.   Theory

61.2.1.   *Peccei-Quinn mechanism and axions* :

The QCD Lagrangian includes a CP-violating term $\mathcal{L}_\Theta = -\bar{\Theta}\,(\alpha_s/8\pi)\,G^{\mu\nu a}\tilde{G}^a_{\mu\nu}$, where $-\pi \leq \bar{\Theta} \leq +\pi$ is the effective Θ parameter after diagonalizing quark masses, $G^a_{\mu\nu}$ is the color field strength tensor, and $\tilde{G}^{a,\mu\nu} \equiv \epsilon^{\mu\nu\lambda\rho}G^a_{\lambda\rho}/2$, with $\varepsilon^{0123} = 1$, its dual. Limits on the neutron electric dipole moment [8] imply $|\bar{\Theta}| \lesssim 10^{-10}$ even though $\bar{\Theta} = \mathcal{O}(1)$ is otherwise completely satisfactory. The spontaneously broken global Peccei-Quinn symmetry $U(1)_{PQ}$ was introduced to solve this "strong CP problem" [1], the axion being the pseudo-NG boson of $U(1)_{PQ}$ [2]. This symmetry is broken due to the axion's anomalous triangle coupling to gluons,

$$\mathcal{L} = \left(\frac{\phi_A}{f_A} - \bar{\Theta}\right)\frac{\alpha_s}{8\pi}\,G^{\mu\nu a}\tilde{G}^a_{\mu\nu}\,, \tag{61.2}$$

where ϕ_A is the axion field and f_A the axion decay constant. Color anomaly factors have been absorbed in the normalization of f_A which is defined by this Lagrangian. Thus normalized, f_A is the quantity that enters all low-energy phenomena [9]. Non-perturbative topological fluctuations of the gluon fields in QCD induce a potential for ϕ_A whose minimum is at $\phi_A = \bar{\Theta}\,f_A$, thereby canceling the $\bar{\Theta}$ term in the QCD Lagrangian and thus restoring CP symmetry.

The resulting axion mass, in units of the PQ scale f_A, is identical to the square root of the topological susceptibility in QCD, $m_A f_A = \sqrt{\chi}$. The latter can be evaluated further [10], exploiting the chiral limit (masses of up and down quarks much smaller than the scale of QCD), yielding $m_A f_A = \sqrt{\chi} \approx f_\pi m_\pi$, where $m_\pi = 135$ MeV and $f_\pi \approx 92$ MeV. In more detail one finds, to next-to-leading order in chiral perturbation theory [11],

$$m_A = 5.70(7)\left(\frac{10^9\,\text{GeV}}{f_A}\right)\text{meV}\,. \tag{61.3}$$

This result was recently confirmed by a direct calculation of the topological susceptibility via QCD lattice simulations [12].

Originally one assumed $f_A \sim v_{\text{weak}}$ [1,2]. Tree-level flavor conservation fixes the axion properties in terms of a single parameter: the ratio of the vacuum expectation values of two Higgs fields that appear as a minimal ingredient. This "standard axion" was excluded after extensive searches [13]. A narrow peak structure observed in positron spectra from heavy ion collisions [14] suggested an axion-like particle of mass 1.8 MeV that decays into e^+e^-, but extensive follow-up searches were negative. "Variant axion models" were proposed which keep $f_A \sim v_{\text{weak}}$ while relaxing the constraint of tree-level flavor conservation [15], but these models are also excluded [16].

However, axions with $f_A \gg v_{\text{weak}}$ evade all current experimental limits. One generic class of models invokes "hadronic axions" where new heavy quarks carry $U(1)_{PQ}$ charges, leaving ordinary quarks and leptons without tree-level axion couplings. The archetype is the KSVZ model [17], where in addition the heavy quarks are electrically neutral.

Another generic class requires at least two Higgs doublets and ordinary quarks and leptons carry PQ charges, the archetype being the DFSZ model [18]. All of these models contain at least one electroweak singlet scalar that acquires a vacuum expectation value and thereby breaks the PQ symmetry. The KSVZ and DFSZ models are frequently used as benchmark examples, but other models exist where both heavy quarks and Higgs doublets carry PQ charges. In supersymmetric models, the axion is part of a supermultiplet and thus inevitably accompanied by a spin-0 saxion and a spin-1 axino, which both also have couplings suppressed by f_A, and are expected to have large masses due to supersymmetry breaking [19].

61.2.2. *Model-dependent axion couplings* :

Although the generic axion interactions scale approximately with f_π/f_A from the corresponding π^0 couplings, there are non-negligible model-dependent factors and uncertainties. The axion's two-photon interaction plays a key role for many searches,

$$\mathcal{L}_{A\gamma\gamma} = -\frac{G_{A\gamma\gamma}}{4} F_{\mu\nu}\tilde{F}^{\mu\nu}\phi_A = G_{A\gamma\gamma}\mathbf{E}\cdot\mathbf{B}\,\phi_A\,, \tag{61.4}$$

where F is the electromagnetic field-strength tensor and $\tilde{F}^{\mu\nu} \equiv \epsilon^{\mu\nu\lambda\rho}F_{\lambda\rho}/2$, with $\varepsilon^{0123} = 1$, its dual. The coupling constant is [11]

$$G_{A\gamma\gamma} = \frac{\alpha}{2\pi f_A}\left(\frac{E}{N} - 1.92(4)\right) = \left(0.203(3)\frac{E}{N} - 0.39(1)\right)\frac{m_A}{\text{GeV}^2}\,, \tag{61.5}$$

where E and N are the electromagnetic and color anomalies of the axial current associated with the axion. In grand unified models, and notably for DFSZ [18], $E/N = 8/3$, whereas for KSVZ [17] $E/N = 0$ if the electric charge of the new heavy quark is taken to vanish. In general, a broad range of E/N values is possible [20], as indicated by the yellow band in Figure 61.1. The two-photon decay width is

$$\Gamma_{A\to\gamma\gamma} = \frac{G_{A\gamma\gamma}^2 m_A^3}{64\,\pi} = 1.1\times 10^{-24}\ \text{s}^{-1}\left(\frac{m_A}{\text{eV}}\right)^5. \tag{61.6}$$

The second expression uses Eq. (1.5) with $E/N = 0$. Axions decay faster than the age of the universe if $m_A \gtrsim 20$ eV.

The interaction with fermions f has derivative form and is invariant under a shift $\phi_A \to \phi_A + \phi_0$ as behooves a NG boson,

$$\mathcal{L}_{Aff} = \frac{C_f}{2f_A}\bar{\Psi}_f\gamma^\mu\gamma_5\Psi_f\partial_\mu\phi_A\,. \tag{61.7}$$

Here, Ψ_f is the fermion field, m_f its mass, and C_f a model-dependent coefficient. The dimensionless combination $g_{Aff} \equiv C_f m_f/f_A$ plays the role of a Yukawa coupling and $\alpha_{Aff} \equiv g_{Aff}^2/4\pi$ of a "fine-structure constant." The often-used pseudoscalar form $\mathcal{L}_{Aff} = -\mathrm{i}\,(C_f m_f/f_A)\,\bar{\Psi}_f\gamma_5\Psi_f\phi_A$ need not be equivalent to the appropriate derivative
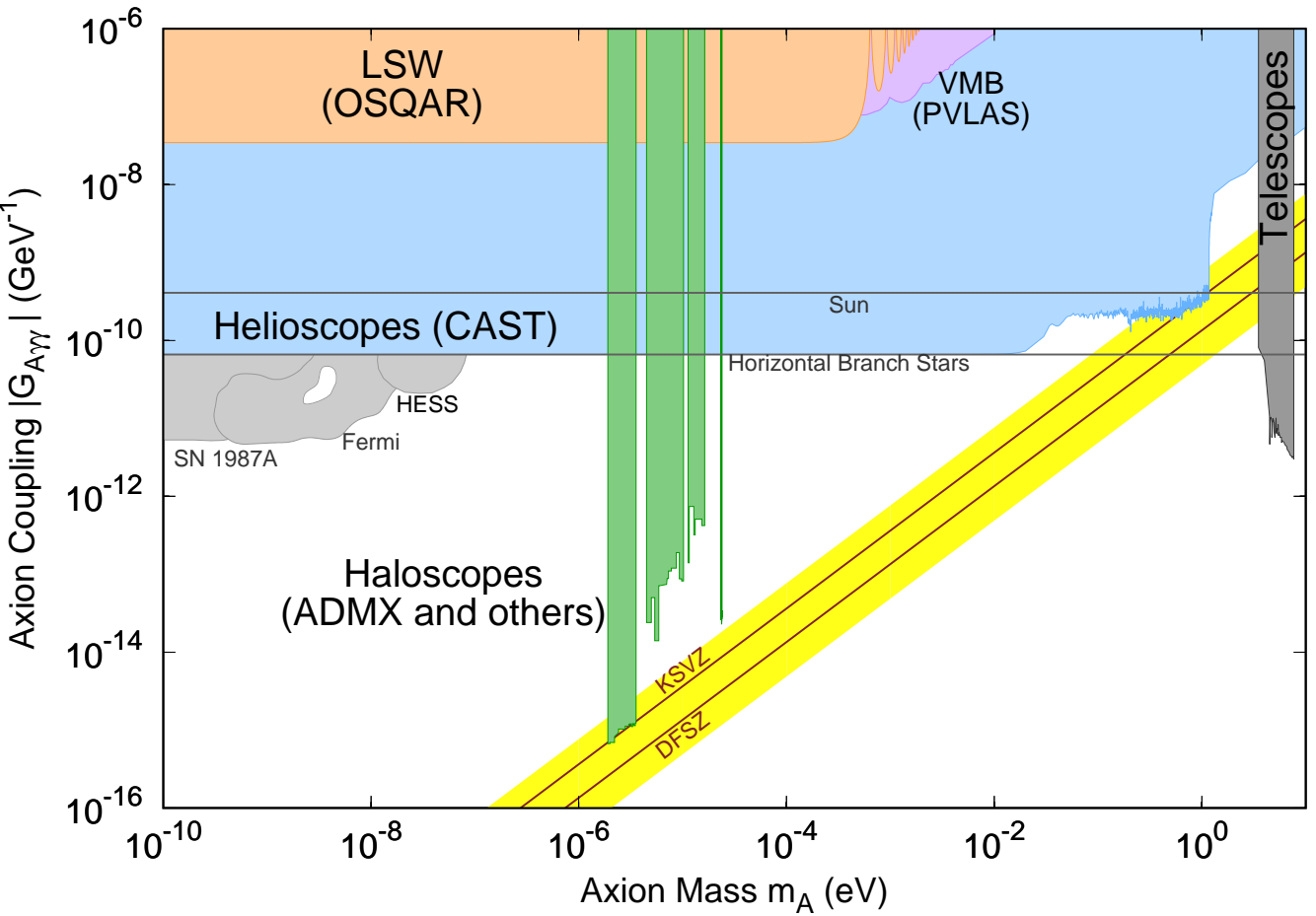
Figure 61.1: Exclusion plot for axion-like particles as described in the text.

structure, for example when two NG bosons are attached to one fermion line as in axion emission by nucleon bremsstrahlung [21].

In the DFSZ model [18], the tree-level coupling coefficient to electrons is [22]

$$C_e = \frac{\sin^2 \beta}{3}, \tag{61.8}$$

where $\tan \beta = v_u/v_d$ is the ratio of the vacuum expectation value v_u of the Higgs field H_u giving masses to the up-type quarks and the vacuum expectation value v_d of the Higgs field H_d giving masses to the down-type quarks.

For nucleons, $C_{n,p}$ have recently been determined as [11]

$$
\begin{aligned}
C_p = {}& -0.47(3) + 0.88(3)C_u - 0.39(2)C_{ad} - 0.038(5)C_s \\
& - 0.012(5)C_c - 0.009(2)C_b - 0.0035(4)C_t, \\
C_n = {}& -0.02(3) + 0.88(3)C_d - 0.39(2)C_u - 0.038(5)C_s \\
& - 0.012(5)C_c - 0.009(2)C_b - 0.0035(4)C_t,
\end{aligned}
\tag{61.9}
$$

in terms of the corresponding model-dependent quark couplings C_q, $q = u, d, s, c, b, t$.

Note, that the model-independent contribution of the neutron is compatible with zero. For hadronic axions $C_q = 0$, so that $C_n = -0.02(3)$. Therefore it is well possible that $C_n = 0$ whereas C_p does not vanish. In the DFSZ model, $C_u = C_c = C_t = \frac{1}{3}\cos^2\beta$ and $C_d = C_s = C_b = \frac{1}{3}\sin^2\beta$, and C_n and C_p, as functions of β,

$$
\begin{aligned}
C_p &= -0.435\sin^2\beta + (-0.182 \pm 0.025)\,, \\
C_n &= 0.414\sin^2\beta + (-0.16 \pm 0.025)\,,
\end{aligned}
\tag{61.10}
$$

do not vanish simultaneously.

The axion-pion interaction is given by the Lagrangian [23]

$$
\mathcal{L}_{A\pi} = \frac{C_{A\pi}}{f_\pi f_A}\left(\pi^0\pi^+\partial_\mu\pi^- + \pi^0\pi^-\partial_\mu\pi^+ - 2\pi^+\pi^-\partial_\mu\pi^0\right)\partial_\mu\phi_A\,,
\tag{61.11}
$$

where $C_{A\pi} = (1-z)/[3(1+z)]$ in hadronic models, with $0.38 < z = m_u/m_d < 0.58$ [24,25]. The chiral symmetry-breaking Lagrangian provides an additional term $\mathcal{L}'_{A\pi} \propto (m_\pi^2/f_\pi f_A)(\pi^0\pi^0 + 2\pi^-\pi^+)\pi^0\phi_A$. For hadronic axions it vanishes identically, in contrast to the DFSZ model (Roberto Peccei, private communication).

61.3. Laboratory Searches

61.3.1. *Light shining through walls* :

Searching for "invisible axions" is extremely challenging due to its extraordinarily feeble coupling to normal matter and radiation. Currently, the most promising approaches rely on the axion-two-photon vertex, allowing for axion-photon conversion in external electric or magnetic fields [5]. For the Coulomb field of a charged particle, the conversion is best viewed as a scattering process, $\gamma + Ze \leftrightarrow Ze + A$, called Primakoff effect [26]. In the other extreme of a macroscopic field, usually a large-scale B-field, the momentum transfer is small, the interaction coherent over a large distance, and the conversion is best viewed as an axion-photon oscillation phenomenon in analogy to neutrino flavor oscillations [27].

Photons propagating through a transverse magnetic field, with incident $\mathbf{E}_\gamma$ and magnet $\mathbf{B}$ parallel, may convert into axions. For $m_A^2 L/2\omega \ll 2\pi$, where L is the length of the B field region and ω the photon energy, the resultant axion beam is coherent with the incident photon beam and the conversion probability is $\Pi \sim (1/4)(G_{A\gamma\gamma}BL)^2$. A practical realization uses a laser beam propagating down the bore of a superconducting dipole magnet (like the bending magnets in high-energy accelerators). If another magnet is in line with the first, but shielded by an optical barrier, then photons may be regenerated from the pure axion beam [28]. The overall probability is $P(\gamma \to A \to \gamma) = \Pi^2$.

The first such experiment utilized two magnets of length $L = 4.4$ m and $B = 3.7$ T and found $|G_{A\gamma\gamma}| < 6.7 \times 10^{-7}$ GeV^{-1} at 95% CL for $m_A < 1$ meV [29]. More recently, several such experiments were performed (see Listings) [30,31]. The current best limit, $|G_{A\gamma\gamma}| < 3.5 \times 10^{-8}$ GeV^{-1} at 95% CL for $m_A \lesssim 0.3$ meV (see Figure 61.1), has been

achieved by the OSQAR (Optical Search for QED Vacuum Birefringence, Axions, and Photon Regeneration) experiment, which exploited two 9 T LHC dipole magnets and an 18.5 W continuous wave laser emitting at the wavelength of 532 nm [31]. Some of these experiments have also reported limits for scalar bosons where the photon $\mathbf{E}_\gamma$ must be chosen perpendicular to the magnet $\mathbf{B}$.

The concept of resonantly enhanced photon regeneration may open unexplored regions of coupling strength [32]. In this scheme, both the production and detection magnets are within Fabry-Perot optical cavities and actively locked in frequency. The $\gamma \to A \to \gamma$ rate is enhanced by a factor $2\mathcal{F}\mathcal{F}'/\pi^2$ relative to a single-pass experiment, where $\mathcal{F}$ and $\mathcal{F}'$ are the finesses of the two cavities. The resonant enhancement could be of order $10^{(10-12)}$, improving the $G_{A\gamma\gamma}$ sensitivity by $10^{(2.5-3)}$. The experiment ALPS II (Any Light Particle Search II) is based on this concept and aims at an improvement of the current laboratory bound on $G_{A\gamma\gamma}$ by a factor $\sim 3 \times 10^3$ in the year 2020 [33].

Resonantly enhanced photon regeneration has already been exploited in experiments searching for "radiowaves shining through a shielding" [34,35]. For $m_A \lesssim 10^{-5}$ eV, the upper bound on $G_{A\gamma\gamma}$ established by the CROWS (CERN Resonant Weakly Interacting sub-eV Particle Search) experiment [36] is slightly less stringent than the one set by OSQAR.

61.3.2. *Photon polarization* :

An alternative to regenerating the lost photons is to use the beam itself to detect conversion: the polarization of light propagating through a transverse B field suffers dichroism and birefringence [37]. Dichroism: The $E_\parallel$ component, but not $E_\perp$, is depleted by axion production, causing a small rotation of linearly polarized light. For $m_A^2 L/2\omega \ll 2\pi$, the effect is independent of m_A. For heavier axions, it oscillates and diminishes as m_A increases, and it vanishes for $m_A > \omega$. Birefringence: This rotation occurs because there is mixing of virtual axions in the $E_\parallel$ state, but not for $E_\perp$. Hence, linearly polarized light will develop elliptical polarization. Higher-order QED also induces vacuum magnetic birefringence (VMB). A search for these effects was performed in the same dipole magnets in the early experiment above [38]. The dichroic rotation gave a stronger limit than the ellipticity rotation: $|G_{A\gamma\gamma}| < 3.6 \times 10^{-7}$ GeV^{-1} at 95% CL for $m_A < 5 \times 10^{-4}$ eV. The ellipticity limits are better at higher masses, as they fall off smoothly and do not terminate at m_A.

In 2006 the PVLAS collaboration reported a signature of magnetically induced vacuum dichroism that could be interpreted as the effect of a pseudoscalar with $m_A = 1$–1.5 meV and $|G_{A\gamma\gamma}| = (1.6$–$5) \times 10^{-6}$ GeV^{-1} [39]. Since then, these findings are attributed to instrumental artifacts [40]. This particle interpretation is also excluded by the above photon regeneration searches that were inspired by the original PVLAS result. Recently, the fourth generation setup of the PVLAS experiment has published new results on searches for VMB (see Figure 61.1) and dichroism [41]. The bounds from the non-observation of the latter on $G_{A\gamma\gamma}$ are slightly weaker than the ones from OSQAR.

61.3.3. *Long-range forces* :

New bosons would mediate long-range forces, which are severely constrained by "fifth force" experiments [42]. Those looking for new mass-spin couplings provide significant constraints on pseudoscalar bosons [43]. Presently, the most restrictive limits are obtained from combining long-range force measurements with stellar cooling arguments [44]. For the moment, any of these limits are far from realistic values expected for axions. Still, these efforts provide constraints on more general low-mass bosons.

Recently, a method was proposed that can extend the search for axion-mediated spin-dependent forces by several orders of magnitude [45]. By combining techniques used in nuclear magnetic resonance and short-distance tests of gravity, this method appears to be sensitive to axions in the μeV – meV mass range, independent of the cosmic axion abundance, if axions have a CP-violating interaction with nuclei as large as the current experimental bound on the electric dipole moment of the neutron allows.

61.4. Axions from Astrophysical Sources

61.4.1. *Stellar energy-loss limits* :

Low-mass weakly-interacting particles (neutrinos, gravitons, axions, baryonic or leptonic gauge bosons, *etc.*) are produced in hot astrophysical plasmas, and can thus transport energy out of stars. The coupling strength of these particles with normal matter and radiation is bounded by the constraint that stellar lifetimes or energy-loss rates not conflict with observation [46–48].

We begin this discussion with our Sun and concentrate on hadronic axions. They are produced predominantly by the Primakoff process $\gamma + Ze \rightarrow Ze + A$. Integrating over a standard solar model yields the axion luminosity [49]

$$L_A = G_{10}^2 \, 1.85 \times 10^{-3} \, L_\odot \,, \tag{61.12}$$

where $G_{10} = |G_{A\gamma\gamma}| \times 10^{10}$ GeV. The maximum of the spectrum is at 3.0 keV, the average at 4.2 keV, and the number flux at Earth is $G_{10}^2 \, 3.75 \times 10^{11}$ cm^{-2} s^{-1}. The solar photon luminosity is fixed, so axion losses require enhanced nuclear energy production and thus enhanced neutrino fluxes. The all-flavor measurements by SNO together with a standard solar model imply $L_A \lesssim 0.10 \, L_\odot$, corresponding to $G_{10} \lesssim 7$ [50], mildly superseding a similar limit from helioseismology [51]. Recently, the limit was improved to $G_{10} < 4.1$ (at $3\,\sigma$), see Figure 61.1 (Sun), exploiting a new statistical analysis that combined helioseismology (sound speed, surface helium and convective radius) and solar neutrino observations, including theoretical and observational errors, and accounting for tensions between input parameters of solar models, in particular the solar element abundances [52].

A more restrictive limit derives from globular-cluster (GC) stars that allow for detailed tests of stellar-evolution theory. The stars on the horizontal branch (HB) in the color-magnitude diagram have reached helium burning with a core-averaged energy release of about 80 erg g^{-1} s^{-1}, compared to Primakoff axion losses of $G_{10}^2 \, 30$ erg g^{-1} s^{-1}. The accelerated consumption of helium reduces the HB lifetime by about $80/(80 + 30 \, G_{10}^2)$.

Number counts of HB stars in a large sample of 39 Galactic GCs compared with the number of red giants (that are not much affected by Primakoff losses) give a weak indication of non-standard losses which may be accounted by Primakoff-like axion emission, if the photon coupling is in the range $|G_{A\gamma\gamma}| = (2.9 \pm 1.8) \times 10^{-11}$ GeV^{-1} [53]. Still, the upper bound found in this analysis,

$$|G_{A\gamma\gamma}| < 6.6 \times 10^{-11} \, \text{GeV}^{-1} \, (95\% \, \text{CL}), \tag{61.13}$$

represents the strongest limit on $G_{A\gamma\gamma}$ for a wide mass range, see Figure 61.1.
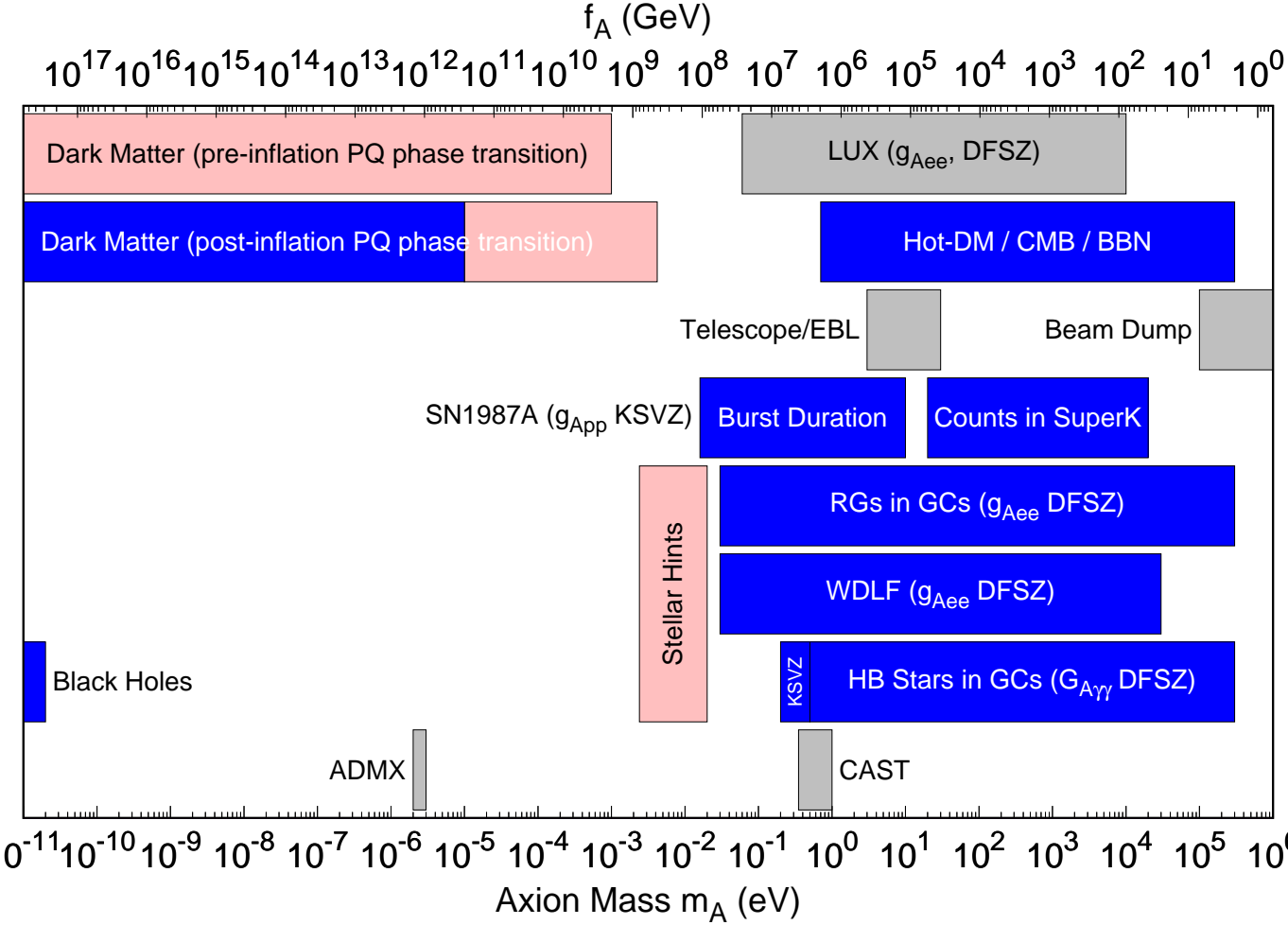

Figure 61.2: Exclusion ranges as described in the text. The intervals in the bottom row are the approximate ADMX and CAST search ranges. Limits on coupling strengths are translated into limits on m_A and f_A using the KSVZ values for the coupling strengths, if not indicated otherwise. The "Beam Dump" bar is a rough representation of the exclusion range for standard or variant axions. The limits for the axion-electron coupling are determined for the DFSZ model with an axion-electron coupling corresponding to $\sin^2 \beta = 1/2$.

We translate the conservative constraint, Equation 61.13, on $G_{A\gamma\gamma}$ to $f_A > 3.4 \times 10^7$ GeV ($m_A < 0.2$ eV), using $E/N = 0$ as in the KSVZ model, and show the excluded range in Figure 61.2. For the DFSZ model with $E/N = 8/3$, the corresponding limits are slightly less restrictive, $f_A > 1.3 \times 10^7$ GeV ($m_A < 0.5$ eV).

If axions couple directly to electrons, the dominant emission processes are atomic axio-recombination and axio-deexcitation, axio-bremsstrahlung in electron-ion or electron-electron collisions, and Compton scattering [54]. Stars in the red giant (RG) branch of the color-magnitude diagram of GCs are particularly sensitive to these processes. In fact, they would lead to an extension of the latter to larger brightness. A recent analysis provided high-precision photometry for the Galactic globular cluster M5 (NGC 5904), allowing for a detailed comparison between the observed tip of the RG branch with predictions based on state-of-the-art stellar evolution theory [55]. It was found that, within the uncertainties, the observed and predicted tip of the RG branch brightness agree reasonably well within uncertainties, leading to the bound

$$\alpha_{Aee} < 1.5 \times 10^{-26} \quad (95\% \text{ CL}), \tag{61.14}$$

implying an upper bound on the axion mass in the DFSZ model,

$$m_A \sin^2 \beta < 15 \text{ meV} \quad (95\% \text{ CL}), \tag{61.15}$$

see Figure 61.2. Intriguingly, the agreement would improve with a small amount of extra cooling that slightly postpones helium ignition, prefering an electron coupling around $\alpha_{Aee} \sim 2.8 \times 10^{-27}$, corresponding to $m_A \sin^2 \beta \sim 7$ meV.

Bremsstrahlung is also efficient in white dwarfs (WDs), where the Primakoff and Compton processes are suppressed by the large plasma frequency. A comparison of the predicted and observed luminosity function of WDs can be used to put limits on α_{Aee} [56]. A recent analysis, based on detailed WD cooling treatment and new data on the WD luminosity function (WDLF) of the Galactic Disk, found that electron couplings above $\alpha_{Aee} \gtrsim 6 \times 10^{-27}$, corresponding to a DFSZ axion mass $m_A \sin^2 \beta \gtrsim 10$ meV, are disfavoured [57], see Figure 61.2. Lower couplings can not be discarded from the current knowledge of the WDLF of the Galactic Disk. On the contrary, features in some WDLFs can be interpreted as suggestions for electron couplings in the range $4.1 \times 10^{-28} \lesssim \alpha_{Aee} \lesssim 3.7 \times 10^{-27}$, corresponding to 2.5 meV $\lesssim m_A \sin^2 \beta \lesssim 7.5$ meV [57,58]. For pulsationally unstable WDs (ZZ Ceti stars), the period decrease $\dot{P}/P$ is a measure of the cooling speed. The corresponding observations of the pulsating WDs G117-B15A and R548 imply additional cooling that can be interpreted also in terms of similar axion losses [59].

Similar constraints derive from the measured duration of the neutrino signal of the supernova SN 1987A. Numerical simulations for a variety of cases, including axions and Kaluza-Klein gravitons, reveal that the energy-loss rate of a nuclear medium at the density 3×10^{14} g cm^{-3} and temperature 30 MeV should not exceed about 1×10^{19} erg g^{-1} s^{-1} [47]. The energy-loss rate from nucleon bremsstrahlung, $N + N \to N + N + A$, is $(C_N/2f_A)^2 (T^4/\pi^2 m_N) F$. Here F is a numerical factor that

represents an integral over the dynamical spin-density structure function because axions couple to the nucleon spin. For realistic conditions, even after considerable effort, one is limited to a heuristic estimate leading to $F \approx 1$ [48]. The SN 1987A limits are of particular interest for hadronic axions where the bounds on α_{Aee} are moot. Using a proton fraction of 0.3, $g_{Ann} = 0$, $F = 1$, and $T = 30$ MeV, one finds $f_A \gtrsim 4 \times 10^8$ GeV and $m_A \lesssim 16$ meV [48], see Figure 61.2. A more detailed numerical calculation [60] with state of the art SN models, again assuming $g_{Ann} = 0$, found that a coupling larger than $|g_{App}| \gtrsim 6 \times 10^{-10}$, would shorten significantly the timescale of the neutrino emission. This result is, not surprisingly, rather close to the estimate in Ref. [48].

The case of a general axion model, interacting with both protons and neutrons, is more complicated. A numerical study in Ref. [61], using the same SN models exploited in Ref. [60], inferred that the combination $g_{App}^2 + g_{Ann}^2$ would be the most appropriate to describe the axion interaction with the nuclear medium, in the regions where the axion emission rate is peaked. In combination with the results in Ref. [60], this suggests the bound

$$g_{App}^2 + g_{Ann}^2 < 3.6 \times 10^{-19} \,. \tag{61.16}$$

Note, however, that no conclusion was drawn in Ref. [60] in terms of a robust constraint from SN 1987A, and that Equation 61.16 should be taken as an indicative result, in absence of a more definite study.

If axions interact sufficiently strongly they are trapped. Only about three orders of magnitude in g_{ANN} or m_A are excluded, a range shown somewhat schematically in Figure 61.2. For even larger couplings, the axion flux would have been negligible, yet it would have triggered additional events in the detectors, excluding a further range [62]. A possible gap between these two SN 1987A arguments was discussed as the "hadronic axion window" under the assumption that $G_{A\gamma\gamma}$ was anomalously small [63]. This range is now excluded by hot dark matter bounds (see below).

There is another hint for excessive stellar energy losses from the neutron star (NS) in the supernova remnant Cassiopeia A (Cas A): its surface temperature measured over 10 years reveals an unusually fast cooling rate. This may be interpreted as a hint for extra cooling by axion neutron bremsstrahlung, requiring a coupling to the neutron of size [64]

$$g_{Ann}^2 = (1.4 \pm 0.5) \times 10^{-19} \tag{61.17}$$

corresponding to an axion mass

$$m_A = (2.3 \pm 0.4)\, \text{meV}/C_n, \tag{61.18}$$

see Figure 61.2. The hint is compatible with the state-of-the-art upper limit on this coupling,

$$g_{Ann}^2 < 6 \times 10^{-19}, \tag{61.19}$$

from NS cooling [65]. In fact, as recently pointed out, the more rapid cooling of the superfluid core in the neutron star may also arise from a phase transition of the neutron condensate into a multicomponent state [66].

Recently, it has been pointed out that the hints of excessive cooling of WDs, RGs and HB stars can be explained at one stroke by an ALP coupling to electrons and photons, with couplings $g_{Aee} \sim 1.5 \times 10^{-13}$ and $|G_{A\gamma\gamma}| \sim 1.4 \times 10^{-11}\,\mathrm{GeV}^{-1}$, respectively [61,67]. Intriguingly, good fits to the data can be obtained employing the DFSZ axion with a mass in the range $2.4\,\mathrm{meV} \lesssim m_A \lesssim 20\,\mathrm{meV}$ ($2\,\sigma$), if the SN 1987A constraint is taken into account [61], see Figure 61.2.

Finally, let us note that if the interpretation of the various hints for additional cooling of stars reported in this section in terms of emission of axions with $m_A \sim \mathrm{meV}$ were correct, SNe would lose a large fraction of their energy as axions. This would lead to a diffuse SN axion background in the universe with an energy density comparable to the extra-galactic background light [68]. However, there is no apparent way of detecting it or the axion burst from the next nearby SN. On the other hand, neutrino detectors such as IceCube, Super-Kamiokande or a future mega-ton water Cerenkov detector will probe exactly the mass region of interest by measuring the neutrino pulse duration of the next galactic SN [60].

61.4.2.   *Searches for solar axions and ALPs* :

Instead of using stellar energy losses to derive axion limits, one can also search directly for these fluxes, notably from the Sun. The main focus has been on axion-like particles with a two-photon vertex. They are produced by the Primakoff process with a flux given by Equation 61.12 and an average energy of 4.2 keV, and can be detected at Earth with the reverse process in a macroscopic B-field ("axion helioscope") [5]. In order to extend the sensitivity in mass towards larger values, one can endow the photon with an effective mass in a gas, $m_\gamma = \omega_{\mathrm{plas}}$, thus matching the axion and photon dispersion relations [69].

An early implementation of these ideas used a conventional dipole magnet, with a conversion volume of variable-pressure gas with a xenon proportional chamber as x-ray detector [70]. The conversion magnet was fixed in orientation and collected data for about 1000 s/day. Axions were excluded for $|G_{A\gamma\gamma}| < 3.6 \times 10^{-9}\ \mathrm{GeV}^{-1}$ for $m_A < 0.03$ eV, and $|G_{A\gamma\gamma}| < 7.7 \times 10^{-9}\ \mathrm{GeV}^{-1}$ for $0.03 < m_A < 0.11$ eV at 95% CL.

Later, the Tokyo axion helioscope used a superconducting magnet on a tracking mount, viewing the Sun continuously. They reported $|G_{A\gamma\gamma}| < 6 \times 10^{-10}\ \mathrm{GeV}^{-1}$ for $m_A < 0.3$ eV [71]. This experiment was recommissioned and a similar limit for masses around 1 eV was reported [72].

The most recent helioscope CAST (CERN Axion Solar Telescope) uses a de-commissioned LHC dipole magnet on a tracking mount. The hardware includes grazing-incidence x-ray optics with solid-state x-ray detectors, as well as a novel x-ray Micromegas position-sensitive gaseous detector. CAST has established a 95% CL limit $|G_{A\gamma\gamma}| < 6.6 \times 10^{-11}\ \mathrm{GeV}^{-1}$ for $m_A < 0.02$ eV [73], exploiting a IAXO (see below) pathfinder system. To cover larger masses, the magnet bores are filled with a gas at varying pressure. The runs with ^{4}He cover masses up to about 0.4 eV [74], providing the ^{4}He limits shown in Figure 61.1. To cover yet larger masses, ^{3}He was used to achieve a larger pressure at cryogenic temperatures. Limits up to 1.17 eV allowed CAST to "cross the axion line" for the KSVZ model [75], see Figure 61.1.

Dark matter direct detection experiments searching for dark matter consisting of weakly interacting massive particles, such as EDELWEISS-II, LUX, and XENON100, have also the capability to search for solar axions and ALPs [76,77]. Recently, the LUX experiment [77] has put a bound on the axion-electron coupling constant by exploiting the axio-electric effect in liquid xenon,

$$g_{Aee} < 3.5 \times 10^{-12} \quad (90\% \text{ CL}), \tag{61.20}$$

excluding the DFSZ model with $m_A \sin^2 \beta > 0.12 \, \text{eV}$, cf. see Figure 61.2.

Going to yet larger masses in a helioscope search is not well motivated because of the cosmic hot dark matter bound of $m_A \lesssim 1$ eV (see below). Sensitivity to significantly smaller values of $G_{A\gamma\gamma}$ can be achieved with a next-generation axion helioscope with a much larger magnetic-field cross section. Realistic design options for this "International Axion Observatory" (IAXO) have been studied in some detail [78]. Such a next-generation axion helioscope may also push the sensitivity in the product of couplings to photons and to electrons, $G_{A\gamma\gamma}g_{Aee}$, into a range beyond stellar energy-loss limits and test the hypothesis that WD, RG, and HB cooling is dominated by axion emission [61,79].

Other Primakoff searches for solar axions and ALPs have been carried out using crystal detectors, exploiting the coherent conversion of axions into photons when the axion angle of incidence satisfies a Bragg condition with a crystal plane [80]. However, none of these limits is more restrictive than the one derived from the constraint on the solar axion luminosity ($L_A \lesssim 0.10 \, L_\odot$) discussed earlier.

Another idea is to look at the Sun with an x-ray satellite when the Earth is in between. Solar axions and ALPs would convert in the Earth magnetic field on the far side and could be detected [81]. The sensitivity to $G_{A\gamma\gamma}$ could be comparable to CAST, but only for much smaller m_A. Deep solar x-ray measurements with existing satellites, using the solar magnetosphere as conversion region, have reported preliminary limits on $G_{A\gamma\gamma}$ [82].

61.4.3. *Conversion of astrophysical photon fluxes* :

Large-scale B fields exist in astrophysics that can induce axion-photon oscillations. In practical cases, B is much smaller than in the laboratory, whereas the conversion region L is much larger. Therefore, while the product BL can be large, realistic sensitivities are usually restricted to very low-mass particles, far away from the "axion band" in a plot like Figure 61.1.

One example is SN 1987A, which would have emitted a burst of axion-like particles (ALPs) due to the Primakoff production in its core. They would have partially converted into γ-rays in the galactic B-field. The lack of a gamma-ray signal in the GRS instrument of the SMM satellite in coincidence with the observation of the neutrinos emitted from SN1987A therefore provides a strong bound on their coupling to photons [83]. Recently, this bound has been revisited and the underlying physics has been brought to the current state-of-the-art, as far as modelling of the supernova and the Milky-Way magnetic field are concerned, resulting in the limit [84]

$$|G_{A\gamma\gamma}| < 5.3 \times 10^{-12} \, \text{GeV}^{-1}, \text{ for } m_A \lesssim 4.4 \times 10^{-10} \, \text{eV}.$$

Magnetically induced oscillations between photons and axion-like particles (ALPs) can modify the photon fluxes from distant sources in various ways, featuring (i) frequency-dependent dimming, (ii) modified polarization, and (iii) avoiding absorption by propagation in the form of axions.

For example, dimming of SNe Ia could influence the interpretation in terms of cosmic acceleration [85], although it has become clear that photon-ALP conversion could only be a subdominant effect [86]. Searches for linearly polarised emission from magnetised white dwarfs [87] and changes of the linear polarisation from radio galaxies (see, e.g., Ref. [88]) provide limits close to $G_{A\gamma\gamma} \sim 10^{-11}$ GeV^{-1}, for masses $m_A \lesssim 10^{-7}$ eV and $m_A \lesssim 10^{-15}$ eV, respectively, albeit with uncertainties related to the underlying assumptions. Even stronger limits, $G_{A\gamma\gamma} \lesssim 2 \times 10^{-13}$ GeV^{-1}, for $m_A \lesssim 10^{-14}$ eV, have been obtained by exploiting high-precision measurements of quasar polarisations [89].

Remarkably, it appears that the universe could be too transparent to TeV γ-rays that should be absorbed by pair production on the extra-galactic background light [90]. The situation is not conclusive at present [91], but the possible role of photon-ALP oscillations in TeV γ-ray astronomy is tantalizing [92]. Fortunately, the region in ALP parameter space, $G_{A\gamma\gamma} \sim 10^{-12} - 10^{-10}$ GeV^{-1} for $m_A \lesssim 10^{-7}$ eV [93], required to explain the anomalous TeV transparency of the universe, could be conceivably probed by the next generation of laboratory experiments (ALPS II) and helioscopes (IAXO) mentioned above. This parameter region can also be probed by searching for an irregular behavior of the gamma ray spectrum of distant active galactic nuclei (AGN), expected to arise from photon-ALP mixing in a limited energy range. The H.E.S.S. collaboration has set a limit of $|G_{A\gamma\gamma}| \lesssim 2.1 \times 10^{-11}$ GeV^{-1}, for 1.5×10^{-8} eV $\lesssim m_A \lesssim 6.0 \times 10^{-8}$ eV, from the non-observation of an irregular behavior of the spectrum of the AGN PKS 2155 [94], see Figure 61.1. Recently, the Fermi-LAT collaboration has put an even more stringent limit on the ALP-photon coupling [95] from observations of the gamma ray spectrum of NGC 1275, the central galaxy of the Perseus cluster, see Figure 61.1.

At smaller masses, $m_A \lesssim 10^{-12}$ eV, galaxy clusters become highly efficient at interconverting ALPs and photons at x-ray energies. Constraints on spectral irregularities in the spectra of luminous x-ray sourced located in or behind galaxy clusters then lead to stringent upper limits on the ALP-photon coupling. Using Chandra and XMM-Newton observations of several local sources in galaxy clusters (Hydra A, M87, NGC 1275, NGC 3862, Seyfert galaxy 2E3140) leads to bounds $|G_{A\gamma\gamma}| \lesssim 1.5 \times 10^{-12}$ GeV^{-1} [96].

61.4.4. *Superradiance of black holes* :

Light bosonic fields such as axions or ALPs can affect the dynamics and gravitational wave emission of rapidly rotating astrophysical black holes through the superradiance mechanism. When their Compton wavelength is of order of the black hole size, they form gravitational bound states around the black hole. Their occupation number grows exponentially by extracting energy and angular momentum from the black hole, forming a coherent axion or ALP bound state emitting gravitational waves. When accretion cannot replenish the spin of the black hole, superradiance dominates the black hole spin evolution; this is true for both supermassive and stellar mass black holes. The existence of destabilizing light bosonic fields thus leads to gaps in the mass vs. spin plot of rotating

black holes. Stellar black hole spin measurements exploiting well-studied binaries and two independent techniques exclude a mass range $6 \times 10^{-13} \, \text{eV} < m_A < 2 \times 10^{-11} \, \text{eV}$ at $2\,\sigma$, which for the axion excludes $3 \times 10^{17} \, \text{GeV} < f_A < 1 \times 10^{19} \, \text{GeV}$ [97]. These bounds apply when gravitational interactions dominate over the axion self-interaction, which is true for the QCD axion in this mass range. Long lasting, monochromatic gravitational wave signals, which can be distinguished from ordinary astrophysical sources by their clustering in a narrow frequency range, are expected to be produced by axions or ALPs annihilating to gravitons. Gravitational waves could also be sourced by axions/ALPs transitioning between gravitationally bound levels. Accordingly, the gravitational wave detector Advanced LIGO should be sensitive to the axion in the $m_A \lesssim 10^{-10} \, \text{eV}$ region. LIGO measurements of black hole spins in binary merger events could also provide statistical evidence for the presence of an axion [98]. Similar signatures could arise for supermassive black holes for particle with masses $\lesssim 10^{-15} \, \text{eV}$. Gravitational waves from such sources could be detected at lower-frequency observatories such as LISA.

61.5.   Cosmic Axions

61.5.1.   *Cosmic axion populations* :

   In the early universe, axions are produced by processes involving quarks and gluons [99]. After color confinement, the dominant thermalization process is $\pi + \pi \leftrightarrow \pi + A$ [23]. The resulting axion population would contribute a hot dark matter component in analogy to massive neutrinos. Cosmological precision data provide restrictive constraints on a possible hot dark-matter fraction that translate into $m_A \lesssim 1$ eV [100], but in detail depend on the used data set and assumed cosmological model. In the future, data from a EUCLID-like survey combined with Planck CMB data can detect hot dark matter axions with a mass $m_A \gtrsim 0.15 \, \text{eV}$ at very high significance [101].

   For $m_A \gtrsim 20$ eV, axions decay fast on a cosmic time scale, removing the axion population while injecting photons. This excess radiation provides additional limits up to very large axion masses [102]. An anomalously small $G_{A\gamma\gamma}$ provides no loophole because suppressing decays leads to thermal axions overdominating the mass density of the universe.

   The main cosmological interest in axions derives from their possible role as cold dark matter (CDM). In addition to thermal processes, axions are abundantly produced by the "re-alignment mechanism" [103].

   The axion dark matter abundance crucially depends on the cosmological history. Let us first consider the so called *pre-inflationary PQ symmetry breaking scenario*, in which the PQ symmetry is broken before and during inflation and not restored afterwards. After the breakdown of the PQ symmetry, the axion field relaxes somewhere in the bottom of the "mexican hat" potential. Near the QCD epoch, topological fluctuations of the gluon fields such as instantons explicitly break the PQ symmetry. This tilting of the "mexican hat" drives the axion field toward the CP-conserving minimum, thereby exciting coherent oscillations of the axion field that ultimately represent a condensate of CDM. The fractional cosmic mass density in this homogeneous field mode, created by

this "vacuum realignment" (vr) mechanism, is [12,104,105,106],

$$\Omega_A^{\mathrm{vr}} h^2 \approx 0.12 \left(\frac{f_A}{9 \times 10^{11} \text{ GeV}} \right)^{1.165} F \bar{\Theta}_{\mathrm{i}}^2$$

$$\approx 0.12 \left(\frac{6 \ \mu\mathrm{eV}}{m_A} \right)^{1.165} F \Theta_{\mathrm{i}}^2 , \qquad (61.21)$$

where h is the present-day Hubble expansion parameter in units of 100 km s^{-1} Mpc^{-1}, and $-\pi \leq \Theta_{\mathrm{i}} \leq \pi$ is the initial "misalignment angle" relative to the CP-conserving position attained in the causally connected region which evolved into today's observable universe. $F = F(\Theta_{\mathrm{i}}, f_A)$ is a factor accounting for anharmonicities in the axion potential. For $F\Theta_{\mathrm{i}}^2 = \mathcal{O}(1)$, m_A should be above $\sim 6\,\mu\mathrm{eV}$ in order that the cosmic axion density does not exceed the observed CDM density, $\Omega_{\mathrm{CDM}} h^2 = 0.12$. However, much smaller axion masses (much higher PQ scales) are still possible if the initial value Θ_{i} just happens to be small enough in today's observable universe ("anthropic axion window" [107]) .

Since the axion field is then present during inflation and thus subject to quantum fluctuations, the non-observation of the associated isocurvature fluctuations in the CMB puts severe constraints in the (f_A, r) plane, where r is the ratio of the power in tensor to the one in scalar fluctuations [108]. In fact, isocurvature constraints, combined with a future measurement of a sizeable r, would strongly disfavor axions with [109]

$$f_A \gtrsim 1.3 \times 10^{13} \, \mathrm{GeV} \left(\frac{r}{0.1} \right)^{1/2} , \ m_A \lesssim 0.4 \ \mu\mathrm{eV} \left(\frac{r}{0.1} \right)^{-1/2} .$$

In the *post-inflationary PQ symmetry breaking scenario*, on the other hand, Θ_{i} will take on different values in different patches of the present universe. The average contribution is [12,104,105,106]

$$\Omega_A^{\mathrm{vr}} h^2 \approx 0.12 \left(\frac{30 \ \mu\mathrm{eV}}{m_A} \right)^{1.165} . \qquad (61.22)$$

However, the presence of cosmic strings can decrease this quantity [106,110]. In fact, the decay of cosmic strings and domain walls gives rise to a different population of cold dark matter axions, whose abundance suffers from significant uncertainties. According to Sikivie and collaborators, these populations are comparable to the re-alignment contribution [111]. Other groups find a significantly enhanced axion density [105,106,112,113] or rather, a larger m_A value for axions providing CDM, namely

$$m_A \approx (50 - 200) \ \mu\mathrm{eV}, \qquad (61.23)$$

for models with short-lived (requiring unit color anomaly $N = 1$) domain walls, such as the KSVZ model. Very recently, a value of $m_A = (26.2 \pm 3.4)\,\mu\mathrm{eV}$ was predicted from an improved calculation including the effect of the large string tension and treating the re-alignment and string-wall contribution in a unified way [110]. For models with long-lived ($N > 1$) domain walls, such as an accidental DFSZ model [114], where the

PQ symmetry is broken by higher dimensional Planck suppressed operators, the mass is predicted to be significantly higher [113,115],

$$m_A \approx (0.6 - 4)\,\mathrm{meV}, \tag{61.24}$$

see Figure 61.2

In this post-inflationary PQ symmetry breakdown scenario, the spatial axion density variations are large at the QCD transition and they are not erased by free streaming. Gravitationally bound "axion miniclusters" form around and before matter-radiation equality [116]. A significant fraction of CDM axions can reside in these bound objects. Remarkably, the minicluster fraction can be bounded by gravitational lensing [117].

In the above predictions of the fractional cosmic mass density in axions, the exponent, 1.165, arises from the non-trivial temperature dependence of the topological susceptibility $\chi(T) = m_A^2(T)f_A^2$ at temperatures slighty above the QCD quark-hadron phase transition. Recent lattice QCD calculations of this exponent [12,118] found it to be remarkably close to the prediction of the dilute instanton gas approximation (see however [119]) which was previously exploited. Therefore, the state-of-the-art prediction of the axion mass relevant for dark matter for a fixed initial misalignment angle Θ_i differs from the previous prediction by just a factor of order one.

The non-thermal production mechanisms attributed to axions are generic to light bosonic weakly interacting particles such as ALPs [120]. The relic abundance is set by the epoch when the axion mass becomes significant, $3H(t) \approx m_A(t)$, and ALP field oscillations begin. For ALPs to contribute to the dark matter density this epoch must occur before matter radiation equality. For a temperature independent ALP mass this leads to the bound:

$$m_A \gtrsim 7 \times 10^{-28}\,\mathrm{eV} \left(\frac{\Omega_m\,h^2}{0.15} \right)^{1/2} \left(\frac{1 + z_{\mathrm{eq}}}{3.4 \times 10^3} \right)^{3/2}. \tag{61.25}$$

ALPs lighter than this bound are allowed if their cosmic energy density is small, but they are quite distinct from other forms of dark matter [121]. Ignoring anharmonicities in the ALP potential, and taking the ALP mass to be temperature independent, the relic density in dark matter ALPs due to re-alignment is given by

$$\Omega_{\mathrm{ALP}}^{\mathrm{vr}}h^2 = 0.12 \left(\frac{m_A}{4.7 \times 10^{-19}\,\mathrm{eV}} \right)^{1/2} \left(\frac{f_A}{10^{16}\,\mathrm{GeV}} \right)^2 \left(\frac{\Omega_m h^2}{0.15} \right)^{3/4} \left(\frac{1 + z_{\mathrm{eq}}}{3.4 \times 10^3} \right)^{-3/4} \Theta_i^2.$$

An ALP decay constant near the GUT scale gives the correct relic abundance for *ultralight ALPs* (ULAs), which we now define. Extended discussions of ULAs can be found in Refs. [122,123].

The standard CDM model treats dark matter as a distribution of cold, collisionless particles interacting only via gravity. Below the Compton wavelength, $\lambda_c = 2\pi/m_A$, the particle description of ALPs breaks down. For large occupation numbers we can model ALPs below the Compton wavelength as a coherent classical field. Taking as a reference

length scale the Earth radius, $R_\oplus = 6371\,\text{km}$, we define ULAs to be those axions with $\lambda_c > R_\oplus$, leading to the defining bound

$$m_{\text{ULA}} < 2 \times 10^{-13}\,\text{eV}\,. \tag{61.26}$$

ULAs encompass the entire Earth in a single coherent field. The coherence time of the ULA field on Earth can be estimated from the crossing time of the de Broglie wavelength at the virial velocity in the Milky Way, $\tau_{\text{coh.}} \sim 1/m_A v_{\text{vir.}}^2$.

We notice that by the definition, Equation 61.26, an ultralight QCD axion must have a super-Planckian decay constant, $f_A > 3 \times 10^{19}\,\text{GeV}$ and would require fine tuning of θ_i to provide the relic abundance. Natural models for ULAs can be found in string and M-theory compactifications [6], in field theory with accidental symmetries [124], or new hidden strongly coupled sectors [125].

In addition to the gravitational potential energy, the ULA field also carries gradient energy. On scales where the gradient energy is non-negligible, ULAs acquire an effective pressure and do not behave as CDM. The gradient energy opposes gravitational collapse, leading to a Jeans scale below which perturbations are stable [126]. The Jeans scale suppresses linear cosmological structure formation relative to CDM [127]. The Jeans scale at matter-radiation equality in the case that ULAs make up all of CDM is:

$$k_{\text{J,eq}} = 8.7\,\text{Mpc}^{-1} \left(\frac{1+z_{\text{eq}}}{3.4 \times 10^3}\right)^{-1/4} \left(\frac{\Omega_{\text{ALP}}^{\text{vr}}}{0.12}\right)^{1/4} \left(\frac{m_A}{10^{-22}\,\text{eV}}\right)^{1/2}$$

On non-linear scales the gradient energy leads to the existence of a class of pseudo-solitons known as oscillatons, or axion stars [128].

Cosmological and astrophysical observations are consistent with the CDM model, and departures from it are only allowed on the scales of the smallest observed dark matter structures with $M \sim 10^{6-8} M_\odot$. The CMB power spectrum and galaxy auto-correlation power spectrum limit the ULA mass to $m_{\text{ULA}} > 10^{-24}\,\text{eV}$ from linear theory of structure formation [121,129]. Analytic models [130] and N-body simulations [131] for non-linear structures show that halo formation is suppressed in ULA models relative to CDM. This leads to constraints on the ULA mass of $m_{\text{ULA}} > 10^{-22}\,\text{eV}$ from observations of high-z galaxies [131,132], and $m_{\text{ULA}} > 10^{-21}\,\text{eV}$ from the Lyman-alpha forest flux power spectrum [133]. Including the effects of anharmonicities on structure formation with ALPs can weaken these bounds if the misalignment angle $\Theta_i \approx \pi$ [134]. Cosmological simulations that treat gradient energy in the ULA field beyond the N-body approximation have just recently become available [135,136], and show, among other things, evidence for the formation of axion stars in the centres of ULA halos. These central axion stars have been conjectured to play a role in the apparently cored density profiles of dwarf spheroidal galaxies [135,137], and may have many other observational consequences [138].

61.5.2.   Telescope searches :

The two-photon decay is extremely slow for axions with masses in the CDM regime, but could be detectable for eV masses. The signature would be a quasi-monochromatic emission line from galaxies and galaxy clusters. The expected optical line intensity for DFSZ axions is similar to the continuum night emission. An early search in three rich Abell clusters [139], and a recent search in two rich Abell clusters [140], exclude the "Telescope" range in Figure 61.1 and Figure 61.2 unless the axion-photon coupling is strongly suppressed. Of course, axions in this mass range would anyway provide an excessive hot DM contribution.

Very low-mass axions in halos produce a weak quasi-monochromatic radio line. Virial velocities in undisrupted dwarf galaxies are very low, and the axion decay line would therefore be extremely narrow. A search with the Haystack radio telescope on three nearby dwarf galaxies provided a limit $|G_{A\gamma\gamma}| < 1.0 \times 10^{-9}$ GeV^{-1} at 96% CL for $298 < m_A < 363$ μeV [141]. However, this combination of m_A and $G_{A\gamma\gamma}$ does not exclude plausible axion models.

61.5.3.   Microwave cavity experiments :

The limits of Figure 61.2 suggest that axions, if they exist, provide a significant fraction or even perhaps all of the cosmic CDM. In a broad range of the plausible m_A range for CDM, galactic halo axions may be detected by their resonant conversion into a quasi-monochromatic microwave signal in a high-Q electromagnetic cavity permeated by a strong static B field [5,142]. The cavity frequency is tunable, and the signal is maximized when the frequency is the total axion energy, rest mass plus kinetic energy, of $\nu = (m_A/2\pi) \left[1 + \mathcal{O}(10^{-6})\right]$, the width above the rest mass representing the virial distribution in the galaxy. The frequency spectrum may also contain finer structure from axions more recently fallen into the galactic potential and not yet completely virialized [143].

The feasibility of this technique was established in early experiments of relatively small sensitive volume, $\mathcal{O}(1$ liter$)$, with HFET-based amplifiers, setting limits in the range $4.5 < m_A < 16.3$ μeV [144], but lacking by 2–3 orders of magnitude the sensitivity required to detect realistic axions. Later, ADMX ($B \sim 8$ T, $V \sim 200$ liters) has achieved sensitivity to KSVZ axions, assuming they saturate the local dark matter density and are well virialized, over the mass range 1.9–3.3 μeV [145]. Should halo axions have a significant component not yet virialized, ADMX is sensitive to DFSZ axions [146]. The corresponding 90% CL exclusion regions shown in Figure 61.3 are normalized to an assumed local CDM density of 7.5×10^{-25} g cm^{-3} (450 MeV cm^{-3}). More recently the ADMX experiment commissioned an upgrade [147] that replaces the microwave HFET amplifiers by near quantum-limited low-noise dc SQUID microwave amplifiers [148], allowing for a significantly improved sensitivity. This apparatus is also sensitive to other hypothetical light bosons, such as hidden photons or chameleons, over a limited parameter space [120,149]. Recently, the HAYSTAC experiment reported on first results from a new microwave cavity search for dark matter axions with masses above 20 μeV. They exclude axions with two-photon coupling $|G_{A\gamma\gamma}| \gtrsim 2 \times 10^{-14}$ GeV^{-1} over the range $23.55\,\mu$eV $< m_A < 24.0\,\mu$eV [150]. Exploiting a Josephson parametric amplifier, this
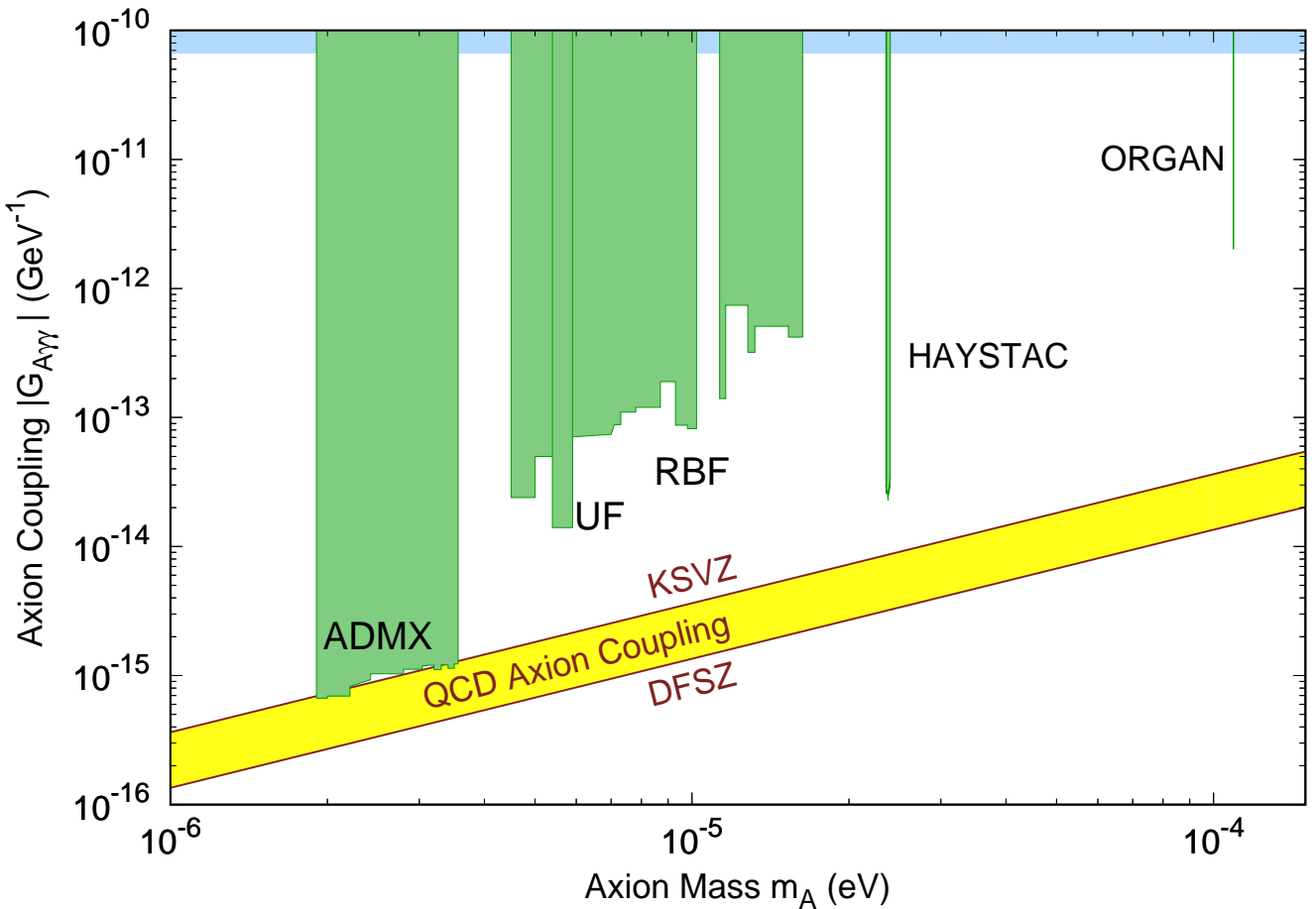
Figure 61.3: Exclusion region reported from the microwave cavity experiments RBF and UF [144], ADMX [145,147], HAYSTAC [150] and ORGAN [152]. A local dark-matter density of 450 MeV cm^{-3} is assumed.

experiment has demonstrated total noise approaching the standard quantum limit for the first time in an axion search. A Rydberg atom single-photon detector [151] can in principle evade the standard quantum limit for coherent photon detection. The ORGAN experiment is designed to probe axions in the mass range $60\,\mu\text{eV} < m_A < 210\,\mu\text{eV}$. In a pathfinding run, it has set a limit on $|G_{A\gamma\gamma}| < 2 \times 10^{-12}\,\text{GeV}^{-1}$ at $110\,\mu\text{eV}$, in a span of $2.5\,\text{neV}$ [152]. There are further microwave cavity axion dark matter experiment in construction (CULTASK [153]) or proposed (KLASH [154]) .

61.5.4. *New concepts for axion dark matter direct detection* :

Other new concepts for searching for axion dark matter are also being investigated. An alternative to the microwave cavity technique is based on a novel detector architecture consisting of an open, Fabry-Perot resonator and a series of current-carrying wire planes [155]. The Orpheus detector has demonstrated this new technique, excluding dark matter ALPs with masses between 68.2 and $76.5\,\mu\text{eV}$ and axion-photon couplings greater than $4 \times 10^{-7}\,\text{GeV}^{-1}$. This technique may be able to probe dark matter axions in the mass range from 40 to $700\,\mu\text{eV}$. Another detector concept exploits the fact that

a magnetized mirror would radiate photons in the background of axion dark matter, which could be collected like in a dish antenna [156]. Searches for hidden photon dark matter exploiting this technique are already underway [157]. The proposed MADMAX experiment will place a stack of dielectric layers in front of the magnetized mirror in order to resonantly enhance the photon signal, aiming a sensitivity to probe the mass range $50\,\mu\mathrm{eV} \lesssim m_A \lesssim 200\,\mu\mathrm{eV}$ [158]. Another proposed axion dark matter search method sensitive in the 100 μeV mass range is to cool a kilogram-sized sample to mK temperatures and count axion induced atomic transitions using laser techniques [159].

The oscillating galactic dark matter axion field induces oscillating nuclear electric dipole moments (EDMs). These EDMs cause the precession of nuclear spins in a nucleon spin polarized sample in the presence of an electric field. The resulting transverse magnetization can be searched for by exploiting magnetic-resonance (MR) techniques, which are most sensitive in the range of low oscillation frequencies corresponding to sub-neV axion masses. The aim of the corresponding Cosmic Axion Spin Precession Experiment (CASPEr) [160] is to probe axion dark matter in the anthropic window, $f_A \gtrsim 10^{15}\,\mathrm{GeV}$, corresponding to $m_A \lesssim \mathrm{neV}$, complementary to the classic axion window probed by the RF cavity technique.

In the intermediate mass region, $\mathrm{neV} \lesssim m_A \lesssim 0.1\,\mu\mathrm{eV}$, one may exploit a cooled LC circuit and precision magnetometry to search for the oscillating electric current induced by dark matter axions in a strong magnetic field [161]. A similar approach is followed by the proposed ABRACADABRA [162] and DM-Radio Pathfinder [163] experiments.

An eventually non-zero axion electron coupling g_{Aee} will lead to an electron spin precession about the axion dark matter wind [164]. The QUAX (QUaerere AXions) experiment aims at exploiting MR inside a magnetized material [165]. Because of the higher Larmor frequency of the electron, it is sensitive in the classic window.

61.6. Conclusions

There is a strengthening physics case for very weakly coupled light particles beyond the Standard Model. The elegant solution of the strong CP problem proposed by Peccei and Quinn yields a particularly strong motivation for the axion. In many theoretically appealing ultraviolet completions of the Standard Model axions and axion-like particles occur automatically. Moreover, they are natural cold dark matter candidates. Perhaps the first hints of their existence have already been seen in the anomalous excessive cooling of stars and the anomalous transparency of the Universe for VHE gamma rays. Interestingly, a significant portion of previously unexplored, but phenomenologically very interesting and theoretically very well motivated axion and ALP parameter space can be tackled in the foreseeable future by a number of terrestrial experiments searching for axion/ALP dark matter, for solar axions/ALPs, and for light apparently shining through a wall.

References:

1. R.D. Peccei and H. Quinn, Phys. Rev. Lett. **38**, 1440 (1977); Phys. Rev. **D16**, 1791 (1977).
2. S. Weinberg, Phys. Rev. Lett. **40**, 223 (1978);
   F. Wilczek, Phys. Rev. Lett. **40**, 279 (1978).
3. F. Wilczek, Phys. Rev. Lett. **49**, 1549 (1982).
4. Y. Chikashige, R.N. Mohapatra, and R.D. Peccei, Phys. Lett. **B98**, 265 (1981);
   G.B. Gelmini and M. Roncadelli, Phys. Lett. **B99**, 411 (1981).
5. P. Sikivie, Phys. Rev. Lett. **51**, 1415 (1983) and Erratum *ibid.*, **52**, 695 (1984).
6. E. Witten, Phys. Lett. **B149**, 351 (1984);
   J.P. Conlon, JHEP **0605**, 078 (2006);
   P. Svrcek and E. Witten, JHEP **0606**, 051 (2006);
   K.-S. Choi *et al.*, Phys. Lett. **B675**, 381 (2009);
   A. Arvanitaki *et al.*, Phys. Rev. **D81**, 123530 (2010);
   B.S. Acharya, K. Bobkov, and P. Kumar, JHEP **1011**, 105 (2010);
   M. Cicoli, M. Goodsell, and A. Ringwald, JHEP **1210**, 146 (2012);
   J. Halverson, C. Long and P. Nath, Phys. Rev. **D96**, 056025 (2017).
7. J. Jaeckel and A. Ringwald, Ann. Rev. Nucl. and Part. Sci. **60**, 405 (2010);
   A. Ringwald, Phys. Dark Univ. **1**, 116 (2012);
   J. Jaeckel, Frascati Phys. Ser. **56**, 172 (2013).
8. C.A. Baker *et al.*, Phys. Rev. Lett. **97**, 131801 (2006).
9. H. Georgi, D.B. Kaplan, and L. Randall, Phys. Lett. **B169**, 73 (1986).
10. R.J. Crewther, Phys. Lett. **B70**, 349 (1977);
    P. Di Vecchia and G. Veneziano, Nucl. Phys. **B171**, 253 (1980).
11. G.G. di Cortona *et al.*, JHEP **1601**, 034 (2016).
12. S. Borsanyi *et al.*, Nature **539**, 69 (2016).
13. T.W. Donnelly *et al.*, Phys. Rev. **D18**, 1607 (1978);
    S. Barshay *et al.*, Phys. Rev. Lett. **46**, 1361 (1981);
    A. Barroso and N.C. Mukhopadhyay, Phys. Lett. **B106**, 91 (1981);
    R.D. Peccei, in *Proceedings of Neutrino '81*, Honolulu, Hawaii, Vol. 1, p. 149 (1981);
    L.M. Krauss and F. Wilczek, Phys. Lett. **B173**, 189 (1986).
14. J. Schweppe *et al.*, Phys. Rev. Lett. **51**, 2261 (1983);
    T. Cowan *et al.*, Phys. Rev. Lett. **54**, 1761 (1985).
15. R.D. Peccei, T.T. Wu, and T. Yanagida, Phys. Lett. **B172**, 435 (1986).
16. W.A. Bardeen, R.D. Peccei, and T. Yanagida, Nucl. Phys. **B279**, 401 (1987).
17. J.E. Kim, Phys. Rev. Lett. **43**, 103 (1979);
    M.A. Shifman, A.I. Vainstein, and V.I. Zakharov, Nucl. Phys. **B166**, 493 (1980).
18. M. Dine, W. Fischler, and M. Srednicki, Phys. Lett. **B104**, 199 (1981);
    A.R. Zhitnitsky, Sov. J. Nucl. Phys. **31**, 260 (1980).
19. J.E. Kim and G. Carosi, Rev. Mod. Phys. **82**, 557 (2010).
20. J.E. Kim, Phys. Rev. **D58**, 055006 (1998);
    L. Di Luzio, F. Mescia and E. Nardi, Phys. Rev. Lett. **118**, 031801 (2017).

21. G. Raffelt and D. Seckel, Phys. Rev. Lett. **60**, 1793 (1988);
     M. Carena and R.D. Peccei, Phys. Rev. **D40**, 652 (1989);
     K. Choi, K. Kang, and J.E. Kim, Phys. Rev. Lett. **62**, 849 (1989).

22. M. Srednicki, Nucl. Phys. **B260**, 689 (1985).

23. S. Chang and K. Choi, Phys. Lett. **B316**, 51 (1993).

24. H. Leutwyler, Phys. Lett. **B378**, 313 (1996).

25. Mini review on Quark Masses in C. Patrignani *et al.* (Particle Data Group), Chin. Phys. C **40**, 100001 (2016).

26. D.A. Dicus *et al.*, Phys. Rev. **D18**, 1829 (1978).

27. G. Raffelt and L. Stodolsky, Phys. Rev. **D37**, 1237 (1988).

28. A.A. Anselm, Yad. Fiz. **42**, 1480 (1985);
     K. van Bibber *et al.*, Phys. Rev. Lett. **59**, 759 (1987).

29. G. Ruoso *et al.*, Z. Phys. **C56**, 505 (1992);
     R. Cameron *et al.*, Phys. Rev. **D47**, 3707 (1993).

30. M. Fouche *et al.* (BMV Collab.), Phys. Rev. **D78**, 032013 (2008);
     P. Pugnat *et al.* (OSQAR Collab.), Phys. Rev. **D78**, 092003 (2008);
     A. Chou *et al.* (GammeV T-969 Collab), Phys. Rev. Lett. **100**, 080402 (2008);
     A. Afanasev *et al.* (LIPSS Collab.), Phys. Rev. Lett. **101**, 120401 (2008);
     K. Ehret *et al.* (ALPS Collab.), Phys. Lett. **B689**, 149 (2010);
     P. Pugnat *et al.* (OSQAR Collab.), Eur. Phys. J. **C74**, 3027 (2014).

31. R. Ballou *et al.* (OSQAR Collab.), Phys. Rev. **D92**, 092002 (2015).

32. F. Hoogeveen and T. Ziegenhagen, Nucl. Phys. **B358**, 3 (1991);
     P. Sikivie, D. Tanner, and K. van Bibber, Phys. Rev. Lett. **98**, 172002 (2007);
     G. Mueller *et al.*, Phys. Rev. **D80**, 072004 (2009).

33. R. Baehre *et al.* (ALPS Collab.), JINST **1308**, T09001 (2013).

34. F. Hoogeveen, Phys. Lett. **B288**, 195 (1992);
     J. Jaeckel and A. Ringwald, Phys. Lett. **B659**, 509 (2008);
     F. Caspers, J. Jaeckel, and A. Ringwald, JINST **0904**, P11013 (2009).

35. R. Povey, J. Hartnett, and M. Tobar, Phys. Rev. **D82**, 052003 (2010);
     A. Wagner *et al.*, Phys. Rev. Lett. **105**, 171801 (2010).

36. M. Betz *et al.*, Phys. Rev. **D88**, 075014 (2013).

37. L. Maiani *et al.*, Phys. Lett. **B175**, 359 (1986).

38. Y. Semertzidis *et al.*, Phys. Rev. Lett. **64**, 2988 (1990).

39. E. Zavattini *et al.* (PVLAS Collab.), Phys. Rev. Lett. **96**, 110406 (2006).

40. E. Zavattini *et al.* (PVLAS Collab.), Phys. Rev. **D77**, 032006 (2008).

41. F. Della Valle *et al.* (PVLAS Collab.), Eur. Phys. J. **C76**, 24 (2016).

42. E. Fischbach and C. Talmadge, Nature **356**, 207 (1992).

43. J.E. Moody and F. Wilczek, Phys. Rev. **D30**, 130 (1984);
     A.N. Youdin *et al.*, Phys. Rev. Lett. **77**, 2170 (1996);
     Wei-Tou Ni *et al.*, Phys. Rev. Lett. **82**, 2439 (1999);
     D.F. Phillips *et al.*, Phys. Rev. **D63**, 111101 (2001);
     B.R. Heckel *et al.* (Eöt-Wash Collab.), Phys. Rev. Lett. **97**, 021603 (2006);
     S.A. Hoedl *et al.*, Phys. Rev. Lett. **106**, 041801 (2011).

44. G. Raffelt, Phys. Rev. **D86**, 015001 (2012).

45. A. Arvanitaki and A.A. Geraci, Phys. Rev. Lett. **113**, 161801 (2014).
46. M.S. Turner, Phys. Reports **197**, 67 (1990);
    G.G. Raffelt, Phys. Reports **198**, 1 (1990).
47. G.G. Raffelt, *Stars as Laboratories for Fundamental Physics*, (Univ. of Chicago Press, Chicago, 1996).
48. G.G. Raffelt, Lect. Notes Phys. **741**, 51 (2008).
49. S. Andriamonje *et al.* (CAST Collab.), JCAP **0704**, 010 (2007).
50. P. Gondolo and G. Raffelt, Phys. Rev. **D79**, 107301 (2009).
51. H. Schlattl, A. Weiss, and G. Raffelt, Astropart. Phys. **10**, 353 (1999).
52. N. Vinyoles *et al.*, JCAP **1510**, 015 (2015).
53. A. Ayala *et al.*, Phys. Rev. Lett. **113**, 191302 (2014);
    O. Straniero *et al.*, doi:10.3204/DESY-PROC-2015-02/straniero_oscar.
54. J. Redondo, JCAP **1312**, 008 (2013).
55. N. Viaux *et al.*, Phys. Rev. Lett. **111**, 231301 (2013).
56. G.G. Raffelt, Phys. Lett. **B166**, 402 (1986);
    S.I. Blinnikov and N.V. Dunina-Barkovskaya, Mon. Not. R. Astron. Soc. **266**, 289 (1994).
57. M.M. Miller Bertolami *et al.*, JCAP **1410**, 069 (2014).
58. J. Isern *et al.*, Astrophys. J. Lett. **682**, L109 (2008);
    J. Isern *et al.*, J. Phys. Conf. Ser. **172**, 012005 (2009).
59. J. Isern *et al.*, Astron. & Astrophys. **512**, A86 (2010);
    A.H. Córsico *et al.*, Mon. Not. Roy. Astron. Soc. **424**, 2792 (2012);
    A.H. Córsico *et al.*, JCAP **1212**, 010 (2012).
60. T. Fischer *et al.*, Phys. Rev. **D94**, 085012 (2016).
61. M. Giannotti *et al.*, JCAP **1710**, 010 (2017).
62. J. Engel, D. Seckel, and A.C. Hayes, Phys. Rev. Lett. **65**, 960 (1990).
63. T. Moroi and H. Murayama, Phys. Lett. **B440**, 69 (1998).
64. L.B. Leinson, JCAP **1408**, 031 (2014).
65. J. Keller and A. Sedrakian, Nucl. Phys. **A897**, 62 (2013);
    A. Sedrakian, Phys. Rev. **D93**, 065044 (2016).
66. L.B. Leinson, Phys. Lett. **B741**, 87 (2015).
67. M. Giannotti *et al.*, JCAP **1605**, 057 (2016).
68. G.G. Raffelt, J. Redondo, and N. Viaux Maira, Phys. Rev. **D84**, 103008 (2011).
69. K. van Bibber *et al.*, Phys. Rev. **D39**, 2089 (1989).
70. D. Lazarus *et al.*, Phys. Rev. Lett. **69**, 2333 (1992).
71. S. Moriyama *et al.*, Phys. Lett. **B434**, 147 (1998);
    Y. Inoue *et al.*, Phys. Lett. **B536**, 18 (2002).
72. M. Minowa *et al.*, Phys. Lett. **B668**, 93 (2008).
73. V. Anastassopoulos *et al.*, Nature Phys. **13**, 584 (2017).
74. E. Arik *et al.* (CAST Collab.), JCAP **0902**, 008 (2009).
75. S. Aune *et al.* (CAST Collab.), Phys. Rev. Lett. **107**, 261302 (2011);
    M. Arik *et al.* (CAST Collab.), Phys. Rev. Lett. **112**, 091302 (2014);
    M. Arik *et al.* (CAST Collab.), Phys. Rev. **D92**, 021101 (2015).

76. E. Armengaud *et al.* (EDELWEISS-II Collab.), JCAP **1311**, 067 (2013);
    E. Aprile *et al.* (XENON100 Collab.), Phys. Rev. **D90**, 062009 (2014) and Erratum
    ibid., **95**,029904(2017).
77. D. S. Akerib *et al.* (LUX Collab.), Phys. Rev. Lett. **118**, 261301 (2017).
78. E. Armengaud *et al.*, JINST **9**, T05002 (2014).
79. K. Barth *et al.*, JCAP **1305**, 010 (2013).
80. F.T. Avignone III *et al.*, Phys. Rev. Lett. **81**, 5068 (1998);
    S. Cebrian *et al.*, Astropart. Phys. **10**, 397 (1999);
    A. Morales *et al.* (COSME Collab.), Astropart. Phys. **16**, 325 (2002);
    R. Bernabei *et al.*, Phys. Lett. **B515**, 6 (2001);
    Z. Ahmed *et al.* (CDMS Collab.), Phys. Rev. Lett. **103**, 141802 (2009);
    E. Armengaud *et al.* (EDELWEISS Collab.), JCAP **1311**, 067 (2013).
81. H. Davoudiasl and P. Huber, Phys. Rev. Lett. **97**, 141302 (2006).
82. H.S. Hudson *et al.*, ASP Conf. Ser. **455**, 25 (2012).
83. J.W. Brockway, E.D. Carlson, and G.G. Raffelt, Phys. Lett. **B383**, 439 (1996);
    J.A. Grifols, E.Massó, and R. Toldrà, Phys. Rev. Lett. **77**, 2372 (1996).
84. A. Payez *et al.*, JCAP **1502**, 006 (2015).
85. C. Csaki, N. Kaloper, and J. Terning, Phys. Rev. Lett. **88**, 161302 (2002).
86. A. Mirizzi, G.G. Raffelt, and P.D. Serpico, Lect. Notes Phys. **741**, 115 (2008).
87. R. Gill and J. S. Heyl, Phys. Rev. **D84**, 085001 (2011).
88. D. Horns *et al.*, Phys. Rev. **D85**, 085021 (2012).
89. A. Payez, J.R. Cudell, and D. Hutsemekers, JCAP **1207**, 041 (2012).
90. D. Horns and M. Meyer, JCAP **1202**, 033 (2012).
91. J. Biteau and D.A. Williams, Astrophys. J. **812**, 60 (2015).
92. A. De Angelis, G. Galanti, and M. Roncadelli, Phys. Rev. **D84**, 105030 (2011);
    M. Simet, D. Hooper, and P.D. Serpico, Phys. Rev. **D77**, 063001 (2008);
    M.A. Sanchez-Conde *et al.*, Phys. Rev. **D79**, 123511 (2009).
93. M. Meyer, D. Horns, and M. Raue, Phys. Rev. **D87**, 035027 (2013).
94. A. Abramowski *et al.* (H.E.S.S. Collab.), Phys. Rev. **D88**, 102003 (2013).
95. M. Ajello *et al.* (Fermi-LAT Collab.), Phys. Rev. Lett. **116**, 161101 (2016).
96. D. Wouters and P. Brun, Astrophys. J. **772**, 44 (2013);
    M. Berg *et al.*, `arXiv:1605.01043` [astro-ph.HE];
    M. C. D. Marsh *et al.*, `arXiv:1703.07354` [hep-ph];
    J. P. Conlon *et al.*, JCAP **1707**, 005 (2017).
97. A. Arvanitaki *et al.*, Phys. Rev. **D81**, 123530 (2010);
    A. Arvanitaki and S. Dubovsky, Phys. Rev. **D83**, 044026 (2011);
    A. Arvanitaki, M. Baryakhtar, and X. Huang, Phys. Rev. **D91**, 084011 (2015).
98. A. Arvanitaki *et al.*, Phys. Rev. **D95**, 043001 (2017).
99. M.S. Turner, Phys. Rev. Lett. **59**, 2489 (1987) and Erratum *ibid.*, **60**, 1101 (1988);
    E. Massó, F. Rota, and G. Zsembinszki, Phys. Rev. **D66**, 023004 (2002);
    P. Graf and F. D. Steffen, Phys. Rev. **D83**, 075011 (2011).
100. S. Hannestad *et al.*, JCAP **1008**, 001 (2010);
    M. Archidiacono *et al.*, JCAP **1310**, 020 (2013);
    E. Di Valentino *et al.*, Phys. Lett. **B752**, 182 (2016).

101. M. Archidiacono *et al.*, JCAP **1505**, 050 (2015).
102. E. Massó and R. Toldra, Phys. Rev. **D55**, 7967 (1997);
     D. Cadamuro and J. Redondo, JCAP **1202**, 032 (2012).
103. J. Preskill, M.B. Wise, and F. Wilczek, Phys. Lett. **B120**, 127 (1983);
     L.F. Abbott and P. Sikivie, Phys. Lett. **B120**, 133 (1983);
     M. Dine and W. Fischler, Phys. Lett. **B120**, 137 (1983).
104. K.J. Bae, J.-H. Huh, and J.E. Kim, JCAP **0809**, 005 (2008).
105. O. Wantz and E.P.S. Shellard, Phys. Rev. **D82**, 123508 (2010).
106. G. Ballesteros, J. Redondo, A. Ringwald and C. Tamarit, JCAP **1708**, 001 (2017).
107. M. Tegmark *et al.*, Phys. Rev. **D73**, 023505 (2006).
108. M. Beltrán, J. García-Bellido, and J. Lesgourgues, Phys. Rev. **D75**, 103507 (2007);
     M.P. Hertzberg, M. Tegmark, and F. Wilczek, Phys. Rev. **D78**, 083507 (2008);
     J. Hamann *et al.*, JCAP **0906**, 022 (2009);
     P.A.R. Ade *et al.* [Planck Collab.], Astron. & Astrophys. **571**, A22 (2014);
     P.A.R. Ade *et al.* [Planck Collab.], Astrophys. Space Sci. **361**, 58 (2016).
109. P. Fox, A. Pierce, and S.D. Thomas, `hep-th/0409059`;
     D.J.E. Marsh *et al.*, Phys. Rev. Lett. **113**, 011801 (2014);
     L. Visinelli and P. Gondolo, Phys. Rev. Lett. **113**, 011802 (2014).
110. V. B. Klaer and G. D. Moore, `arXiv:1708.07521` [hep-ph].
111. S. Chang, C. Hagmann and P. Sikivie, Phys. Rev. **D59**, 023505 (1999);
     C. Hagmann, S. Chang and P. Sikivie, Phys. Rev. **D63**, 125018 (2001).
112. T. Hiramatsu *et al.*, Phys. Rev. **D83**, 123531 (2011);
     T. Hiramatsu *et al.*, Phys. Rev. **D85**, 105020 (2012) and Erratum *ibid.*, **86**, 089902 (2012).
113. M. Kawasaki, K. Saikawa, and T. Sekiguchi, Phys. Rev. **D91**, 065014 (2015).
114. A. Ringwald and K. Saikawa, Phys. Rev. **D94**, 049908 (2016) and Addendum *ibid.*, **94**, 049908 (2016).
115. T. Hiramatsu, M. Kawasaki, K. Saikawa and T. Sekiguchi, JCAP **1301**, 001 (2013).
116. E.W. Kolb and I.I. Tkachev, Phys. Rev. Lett. **71**, 3051 (1993);
     K.M. Zurek, C.J. Hogan, and T.R. Quinn, Phys. Rev. **D75**, 043511 (2007).
117. E.W. Kolb and I.I. Tkachev, Astrophys. J. **460**, L25 (1996);
     M. Fairbairn, D. J. E. Marsh and J. Quevillon, Phys. Rev. Lett. **119**, 021101 (2017).
118. E. Berkowitz, M. I. Buchoff and E. Rinaldi, Phys. Rev. **D92**, 034507 (2015);
     S. Borsanyi *et al.*, Phys. Lett. **B752**, 175 (2016);
     R. Kitano and N. Yamada, JHEP **1510**, 136 (2015);
     P. Petreczky, H. P. Schadler and S. Sharma, Phys. Lett. **B762**, 498 (2016);
     Y. Taniguchi *et al.*, Phys. Rev. **D95**, 054502 (2017).
119. C. Bonati *et al.*, JHEP **1603**, 155 (2016).
120. P. Arias *et al.*, JCAP **1206**, 013 (2012).
121. R. Hlozek *et al.*, Phys. Rev. **D91**, 103512 (2015).
122. D. J. E. Marsh, Phys. Rept. **643**, 1 (2016).
123. L. Hui, J. P. Ostriker, S. Tremaine and E. Witten, Phys. Rev. **D95**, 043541 (2017).

124. A. G. Dias *et al.*, JHEP **1406**, 037 (2014);
J. E. Kim and D. J. E. Marsh, Phys. Rev. **D93**, 025027 (2016).
125. H. Davoudiasl and C. W. Murphy, Phys. Rev. Lett. **118**, 141801 (2017).
126. M. Khlopov *et al.*, Mon. Not. Roy. Astron. Soc. **215**, 575 (1985)..
127. W. Hu, R. Barkana and A. Gruzinov, Phys. Rev. Lett. **85**, 1158 (2000);
L. Amendola and R. Barbieri, Phys. Lett. **B642**, 192 (2006);
D. J. E. Marsh and P. G. Ferreira, Phys. Rev. **D82**, 103528 (2010).
128. E. Seidel and W. M. Suen, Phys. Rev. Lett. **66**, 1659 (1991).
129. R. Hlozek, D. J. E. Marsh and D. Grin, `arXiv:1708.05681` [astro-ph.CO].
130. D. J. E. Marsh and J. Silk, Mon. Not. Roy. Astron. Soc. **437**, 2652 (2014).
131. H. Y. Schive, T. Chiueh, T. Broadhurst and K. W. Huang, Astrophys. J. 818,89(2016).
132. B. Bozek *et al.*, Mon. Not. Roy. Astron. Soc. **450**, 209 (2015);
P. S. Corasaniti, *et al.*, Phys. Rev. **D95**, 083512 (2017).
133. E. Armengaud *et al.*, Mon. Not. Roy. Astron. Soc. **471**, 4606 (2017);
V. Irsic *et al.*, Phys. Rev. Lett. **119**, 031302 (2017);
T. Kobayashi *et al.*, `arXiv:1708.00015` [astro-ph.CO].
134. H. Y. Schive and T. Chiueh, `arXiv:1706.03723` [astro-ph.CO].
135. H. Y. Schive, T. Chiueh and T. Broadhurst, Nature Phys. **10**, 496 (2014).
136. B. Schwabe, J. C. Niemeyer and J. F. Engels, Phys. Rev. **D94**, 043513 (2016);
J. Veltmaat and J. C. Niemeyer, Phys. Rev. **D94**, 123523 (2016);
P. Mocz *et al.*, `1705.05845` [astro-ph.CO].
137. D. J. E. Marsh and A. R. Pop, Mon. Not. Roy. Astron. Soc. **451**, 2479 (2015);
S. R. Chen *et al.*, Mon. Not. Roy. Astron. Soc. **468**, 1338 (2017);
A. X. Gonzles-Morales *et al.*, Mon. Not. Roy. Astron. Soc. **472**, 1346 (2017).
138. D. G. Levkov, A. G. Panin and I. I. Tkachev, Phys. Rev. Lett. **118**, 011301 (2017);
T. Helfer *et al.*, JCAP **1703**, 055 (2017);
J. Eby, M. Ma, P. Suranyi and L. C. R. Wijewardhana, `1705.05385` [hep-ph].
139. M. Bershady *et al.*, Phys. Rev. Lett. **66**, 1398 (1991);
M. Ressell, Phys. Rev. **D44**, 3001 (1991).
140. D. Grin *et al.*, Phys. Rev. **D75**, 105018 (2007).
141. B.D. Blout *et al.*, Astrophys. J. **546**, 825 (2001).
142. P. Sikivie, Phys. Rev. **D32**, 2988 (1985);
L. Krauss *et al.*, Phys. Rev. Lett. **55**, 1797 (1985);
R. Bradley *et al.*, Rev. Mod. Phys. **75**, 777 (2003).
143. P. Sikivie and J. Ipser, Phys. Lett. **B291**, 288 (1992);
P. Sikivie *et al.*, Phys. Rev. Lett. **75**, 2911 (1995).
144. S. DePanfilis *et al.*, Phys. Rev. Lett. **59**, 839 (1987);
W. Wuensch *et al.*, Phys. Rev. **D40**, 3153 (1989);
C. Hagmann *et al.*, Phys. Rev. **D42**, 1297 (1990).
145. S. Asztalos *et al.*, Phys. Rev. **D69**, 011101 (2004).
146. L. Duffy *et al.*, Phys. Rev. Lett. **95**, 091304 (2005);
J. Hoskins *et al.*, Phys. Rev. **D84**, 121302 (2011).
147. S.J. Asztalos *et al.* (ADMX Collab.), Phys. Rev. Lett. **104**, 041301 (2010).

148. S.J. Asztalos *et al.*, Nucl. Instrum. Methods **A656**, 39 (2011).
149. G. Rybka *et al.*, Phys. Rev. Lett. **105**, 051801 (2010);
     A. Wagner *et al.*, Phys. Rev. Lett. **105**, 171801 (2010).
150. B. M. Brubaker *et al.*, Phys. Rev. Lett. **118**, 061302 (2017).
151. I. Ogawa, S. Matsuki, and K. Yamamoto, Phys. Rev. **D53**, 1740 (1996);
     Y. Kishimoto *et al.*, Phys. Lett. **A303**, 279 (2002);
     M. Tada *et al.*, Phys. Lett. **A303**, 285 (2002);
     T.Haseyama *et al.*, J. Low Temp. Phys. **150**, 549 (2008).
152. B. T. McAllister *et al.*, `arXiv:1706.00209` [physics.ins-det].
153. W. Chung, PoS CORFU **2015**, 047 (2016).
154. D. Alesini *et al.*, `arXiv:1707.06010` [physics.ins-det].
155. G. Rybka *et al.*, Phys. Rev. **D91**, 011701 (2015).
156. D. Horns *et al.*, JCAP **1304**, 016 (2013).
157. J. Suzuki *et al.*, JCAP **1509**, 042 (2015);
     B. Döbrich *et al.*, `arXiv:1510.05869` [physics.ins-det].
158. A. Caldwell *et al.*[MADMAX Working Group], Phys. Rev. Lett. **118**, 091801 (2017).
159. P. Sikivie, Phys. Rev. Lett. **113**, 201301 (2014).
160. D. Budker *et al.*, Phys. Rev. **X4**, 021030 (2014).
161. P. Sikivie, N. Sullivan, and D. B. Tanner, Phys. Rev. Lett. **112**, 131301 (2014).
162. Y. Kahn, B. R. Safdi and J. Thaler, Phys. Rev. Lett. **117**, 141801 (2016).
163. M. Silva-Feaver *et al.*, `arXiv:1610.09344` [astro-ph.IM].
164. L. Krauss *et al.*, Phys. Rev. Lett. **55**, 1797 (1985);
     R. Barbieri *et al.*, Phys. Rev. **B226**, 357 (1989).
165. R. Barbieri *et al.*, Phys. Dark Univ. **15**, 135 (2017).